frontiers in Cardiovascular Medicine

REVIEW
published: 18 January 2022
doi: 10.3389/fcvm.2021.794706

A Clinical Approach to Multimodality Imaging in Pulmonary Hypertension

Christine Farrell[1†], *Aparna Balasubramanian*[2†], *Allison G. Hays*[3], *Steven Hsu*[3], *Steven Rowe*[4], *Stefan L. Zimmerman*[4], *Paul M. Hassoun*[1], *Stephen C. Mathai*[2] *and Monica Mukherjee*[3*]

[1] Division of Medicine, Johns Hopkins University, Baltimore, MD, United States, [2] Division of Pulmonary and Critical Care Medicine, Johns Hopkins University, Baltimore, MD, United States, [3] Division of Cardiology, Johns Hopkins University, Baltimore, MD, United States, [4] Division of Radiology, Johns Hopkins University, Baltimore, MD, United States

Pulmonary hypertension (PH) is a clinical condition characterized by progressive elevations in mean pulmonary artery pressures and right ventricular dysfunction, associated with significant morbidity and mortality. For resting PH to develop, ∼50–70% of the pulmonary vasculature must be affected, suggesting that even mild hemodynamic abnormalities are representative of advanced pulmonary vascular disease. The definitive diagnosis of PH is based upon hemodynamics measured by right heart catheterization; however this is an invasive and resource intense study. Early identification of pulmonary vascular disease offers the opportunity to improve outcomes by instituting therapies that slow, reverse, or potentially prevent this devastating disease. Multimodality imaging, including non-invasive modalities such as echocardiography, computed tomography, ventilation perfusion scans, and cardiac magnetic resonance imaging, has emerged as an integral tool for screening, classifying, prognosticating, and monitoring response to therapy in PH. Additionally, novel imaging modalities such as echocardiographic strain imaging, 3D echocardiography, dual energy CT, FDG-PET, and 4D flow MRI are actively being investigated to assess the severity of right ventricular dysfunction in PH. In this review, we will describe the utility and clinical application of multimodality imaging techniques across PH subtypes as it pertains to screening and monitoring of PH.

Keywords: pulmonary hypertension, echocardiography, computed tomography, scintigraphy, magnetic resonance imaging

OPEN ACCESS

Edited by:
Erhan Tenekecioglu,
University of Health Sciences, Turkey

Reviewed by:
Francesco Sturla,
IRCCS Policlinico San Donato, Italy
Keiichi Hirono,
University of Toyama, Japan

***Correspondence:**
Monica Mukherjee
mmukher2@jhu.edu

[†] These authors share first authorship

Specialty section:
This article was submitted to Cardiovascular Imaging, a section of the journal Frontiers in Cardiovascular Medicine

Received: *14 October 2021*
Accepted: *22 November 2021*
Published: *18 January 2022*

Citation:
Farrell C, Balasubramanian A, Hays AG, Hsu S, Rowe S, Zimmerman SL, Hassoun PM, Mathai SC and Mukherjee M (2022) A Clinical Approach to Multimodality Imaging in Pulmonary Hypertension. Front. Cardiovasc. Med. 8:794706. doi: 10.3389/fcvm.2021.794706

KEY POINTS

- Pulmonary hypertension is a devastating disease and early detection improves morbidity and mortality.
- Echocardiography, computed tomography, nuclear imaging, and magnetic resonance imaging are non-invasive imaging studies for screening, classification, prognostication, and monitoring of pulmonary hypertension.
- New non-invasive imaging techniques such as strain imaging, 3D echocardiography, dual energy CT, and 4D flow MRI are emerging techniques that can assist in the diagnosis and monitoring of pulmonary hypertension.

INTRODUCTION

Pulmonary hypertension (PH) is an insidious, highly morbid, and heterogeneous disease that is characterized by elevations in pulmonary arterial pressures and is classified into five groups based on etiology (1–3). Early diagnosis and referral are associated with better clinical outcomes, however the time from symptom onset to diagnosis is often greater than 2 years (4–6). PH is exclusively diagnosed using confirmatory invasive right heart catheterization (RHC) to measure mean pulmonary artery pressure (mPAP), pulmonary capillary wedge pressure (PCWP), and pulmonary vascular resistance (PVR) (7). Currently, PH is defined by a mPAP >20 mmHg, a threshold which was recently decreased from ≥25 mmHg based on epidemiologic data demonstrating the distribution of mPAP among healthy individuals and the significant impact of mildly elevated pulmonary pressures on morbidity and mortality (8).

While RHC is the only method to directly measure pulmonary and right heart pressures, it is invasive, resource intensive, and carries procedural risk (9). As a result, in 2015, the European Society of Cardiology/European Respiratory Society guidelines recommended the use of a variety of non-invasive imaging modalities to screen and risk stratify patients (10). The standard of care for screening and classifying PH includes transthoracic echocardiogram (TTE), chest computed tomography (CT), ventilation perfusion (VQ) scan, RHC, and increasingly cardiac magnetic resonance imaging (CMR). Multimodality imaging is useful for screening, classifying, prognosticating, and monitoring effectiveness of therapy in PH. This review seeks to describe the current imaging modalities used in diagnosing and monitoring the various forms of PH along with several novel imaging modalities that may soon be incorporated into clinical practice.

METHODOLOGY

We conducted a search utilizing Medline/PubMed from November 1989 to June 2021 to identify relevant articles. Search terms included: pulmonary hypertension AND echocardiography OR magnetic resonance OR computed tomography OR nuclear OR cardiovascular imaging. Identified articles were then evaluated, including screening of references. Review articles, meta-analyses, and major medical society guideline documents were also assessed. Finally, selected articles were included if felt to be relevant in the authors' opinion. Data from these articles were abstracted and guided this narrative review.

RESULTS

We identified 46 articles on echocardiography, 19 on computerized tomography, 7 on nuclear medicine techniques including scintigraphy, and 45 on magnetic resonance imaging in PH.

Echocardiography

TTE is the most common imaging modality used to screen for PH and is the mainstay for screening, monitoring of therapeutic response, and prognostication (11). As most deaths from PH are from right heart failure, recognizing the presence, and quantifying the degree of right heart dysfunction, is helpful in monitoring disease progression and prognostication. In addition to conventional two-dimensional (2D) TTE, speckle-tracking strain imaging and three-dimensional (3D) echocardiography are more specialized techniques that are increasingly becoming part of the standard of care in monitoring right heart structure and function. Representative echocardiographic images are shown in **Figure 1**.

Screening for Pulmonary Hypertension

Screening for PH using conventional TTE primarily relies upon assessment of the right ventricular systolic pressure (RVSP), which is measured from the tricuspid regurgitant (TR) jet velocity and size/collapsibility of the inferior vena cava (IVC) to estimate right atrial pressure (RAP) (12). Using the modified Bernoulli equation, $RVSP = 4V^2 + RAP$ with V equaling the maximum TR jet velocity (13). For RVSP measurements > 40 mmHg, a right heart catherization is recommended (14). However, RVSP has been shown in numerous studies across various PH subgroups to poorly correlate with systolic pulmonary artery pressure (sPAP) measured by RHC. These studies have routinely shown that RVSP is ± 10 mmHg different to the true sPAP in approximately 50% of cases (15–18). Additionally, the ability to capture and quantify the TR jet velocity can be technically challenging and is estimated to be feasible in only 75% of cases (19). RVSP can be combined with other non-invasive measures to evaluate the need for a RHC in suspected PH (20). Additional RV hemodynamics can also be obtained including PA end-diastolic pressure using end-diastolic pulmonic regurgitation peak velocity, mean PA pressure, and pulmonary vascular resistance. Lastly, early closure of the pulmonic valve due to rapid pressure equilibration of the RV and PA in midsystole can be detected using both M-mode or pulse waved Doppler signal, known as the "flying W" sign (21).

Assessment of the Right Heart

The American Society of Echocardiography has standardized measurements of right-sided cardiac structure and function (13). Measurements include the right atrial and ventricular area, fractional area change (FAC) as a surrogate of right ventricular ejection fraction (RVEF), tricuspid annular plane systolic excursion (TAPSE), RVSP, and the presence of a pericardial effusion. A right atrial area measured at the end of systole >18 cm^2 has been independently associated with elevated right ventricular (RV) end-diastolic pressure (RVEDP) and mean RAP with a sensitivity of 89% and specificity of 82% (13, 22). The RV diameter at the base is considered enlarged when it is >42 mm. However, this measure only weakly correlates with the gold standard RV volume assessment *via* CMR (23, 24). Measurements based off estimations of the 2D RV area or volume, such as FAC or RVEF, are similarly flawed when compared to CMR techniques (25, 26) due to the complex shape of the right ventricle (27). Eccentricity index, or interventricular septal morphology, is a useful echocardiographic tool and assesses the interventricular dependency of the RV:LV from the parasternal short-axis view and is an important component of the

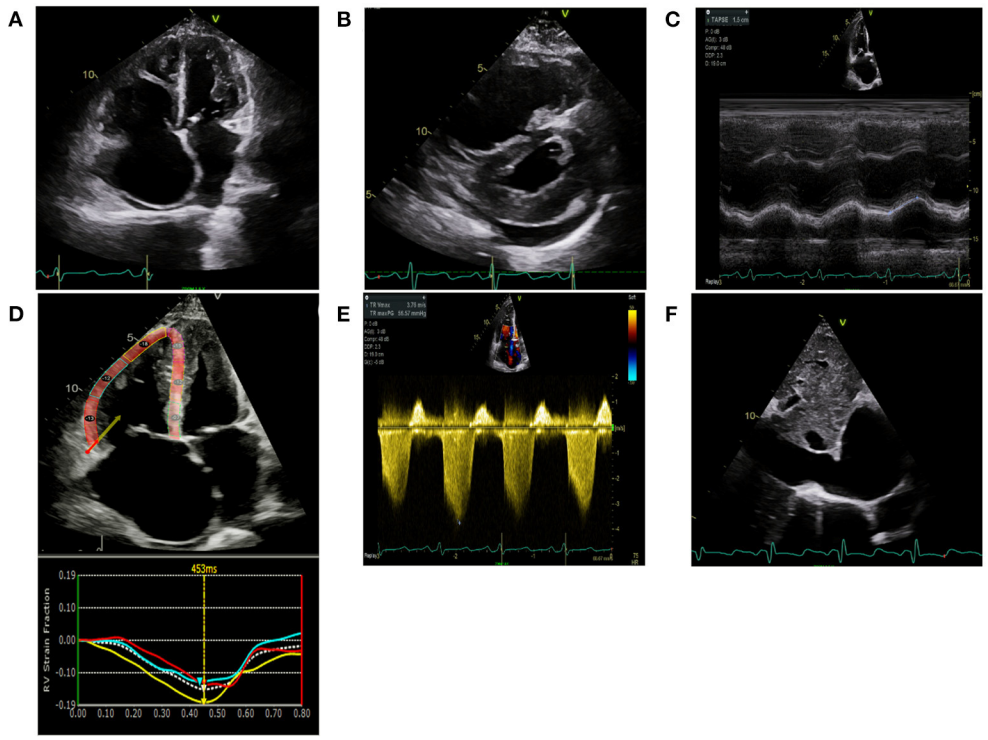

FIGURE 1 | Echocardiographic images are shown in a scleroderma patient with severe pulmonary hypertension on stable therapies. **(A)** Apical 4 chamber view demonstrates severe right atrial enlargement with bowing of the interatrial septum from right to left suggestive of elevated right atrial pressures. The right ventricle is severely dilated and hypertrophied with a prominent moderator band. The left ventricle is hypertrophied and small. **(B)** Parasternal short-axis is shown in the same patient with marked RV enlargement and evidence of RV pressure overload distorting the normal circular short-axis geometry of the LV. There is a small posterior pericardial effusion present. **(C)** Tricuspid annular plane systolic excursion (TAPSE) utilizes M-mode techniques to measure the longitudinal motion of the basal right ventricular wall segment during systole as an estimate of right ventricular systolic function. TAPSE is mildly reduced at 1.5 cm (normal >1.6 cm) however fractional area change was 24% (moderate-severely reduced). **(D)** Right Ventricular Longitudinal Systolic Strain (RVLSS) is a recent echocardiographic advancement based on ultrasound-myocardial tissue interactions. Each segment of the RV in this example corresponds with a strain curve with the white dotted line representing an average of the segmental strain for the regional curves in this view. Regional RV free wall strain is reduced in the basal and midventricular wall segments with less reduction in the apical segment. Global strain is an average of the three RV free wall segments and is −14.3%. **(E)** Right Ventricular Systolic Pressure utilizes the peak tricuspid velocity to calculate the peak right ventricular systolic pressure using the modified Bernoulli equation. RVSP= [peak gradient (mmHg) = right atrial pressure + (4 × Peak velocity 2)]. In this example, RVSP = 57 mmHg + 15 mmHg = 72 mmHg. **(F)** Right atrial pressures are estimated from the IVC diameter made in subcostal view at end-expiration. In this example, the IVC is severely dilated at 3.2 cm with minimal respiratory variation suggestive of markedly elevated right atrial pressure of 15 mmHg.

ESC/ERS recommendations for PH screening (11). The presence of RV hypertrophy may also be seen in chronic pressure/volume overload states.

Due to the inaccuracy of RV area and volume assessments using 2D echocardiographic techniques, other measurements are used to estimate RV function. Tricuspid annular plane systolic excursion (TAPSE) measures the movement of the tricuspid annulus toward the apex between diastole and systole in M-mode. A measurement ≤1.7 cm is considered abnormal (28). TAPSE has been shown to closely correlate with RVEF on CMR and RHC (29). However, TAPSE measurements should be interpreted with caution in patients with severe TR as they have been shown to be less accurate in that setting (30). The Tei index, or myocardial performance index (MPI) of the RV, is measured using either color or tissue Doppler imaging and is a ratio of isovolumic time, both in contraction and relaxation, to ejection time (31, 32). Systolic wave velocity (S′) is another measure of myocardial contraction measured from tissue Doppler imaging and has been validated in an epidemiologic study of healthy individuals to define normal values (33). Abnormal tissue Doppler S′ velocity is defined as <9.5 cm/s.

Prognostication

As right heart failure is the primary cause of death among individuals with PH, assessment of abnormalities in the right ventricle by echocardiogram offers significant prognostic information. RA area and estimation of right atrial pressure have been demonstrated to be associated with mortality secondary to right heart failure (34). RVSP has been found to be an independent predictor of mortality in PH (35, 36) and while neither sensitive nor specific, the presence of a pericardial effusion has been shown to predict mortality in PH patients (34, 37, 38).

Recently, the REVEAL registry has included echocardiographic assessment of pericardial effusion in prognostic risk assessment of PAH (REVEAL risk score). Regarding RV functional assessments in individuals with known PH, reduced TAPSE has been shown to have a nearly four-fold increased risk of death (39) with every 1 mm decrease in TAPSE increasing the unadjusted risk of death by 17% (40). Myocardial performance index is associated with clinical status and mortality, as well as change in clinical status over time in response to therapy (31, 41).

Speckle-Tracking Echocardiography (Echo Strain Imaging)

Strain imaging is being increasingly incorporated into clinical practice as a measurement of RV systolic function (42). Strain (ε) is the deformation of cardiac tissue from an applied force with $\varepsilon = (L_{systole}\text{-}L_{diastole})/L_{diastole}$ with L being length (42) and multiplied by 100 resulting in a percentage of myocardial deformation across the cardiac cycle. A positive number indicates lengthening, and a negative number indicates shortening. Strain imaging provides a feasible non-invasive technique to assess cardiac mechanics for the detection of subclinical ventricular dysfunction.

Using 2D echocardiographic techniques, there are two methods by which strain can be calculated: tissue Doppler imaging (TDI) and speckle tracking echocardiography (STE). TDI-derived strain calculates the rate at which a particular segment of the myocardium moves toward or away from the transducer (43). TDI is less commonly used since it is highly angle dependent and requires high frame rates. In contrast, STE is angle-independent and performed by measuring the movement, or deformation, of ultrasound pixels over the cardiac cycle. It is particularly helpful in the right heart as it tends to preferentially measure speckles at the endocardial border whose longitudinal fibers account for 80% of RV contraction. STE-derived strain can be reported across the RV free wall regions or as an average of visualized segments known as global longitudinal strain (GLS) and is expressed as a percentage and a more negative number signifies a more shortening of the myocardial segment during systole. Worsening strain refers to a less negative number (a lower absolute value) than expected or diminished deformation along the longitudinal axis. GLS typically represents the basal, midventricular, and apical RV free segments however it may also include the basal, midventricular, and apical segments of the interventricular septum. The latter approach, however, is less favored due to inability to isolate RV and LV contributions (42). The most common measurement of strain in the RV is GLS, however individual longitudinal segmental strain is also being investigated in PH (44).

Reduced RV function using STE GLS imaging predicts worse clinical outcomes such as right heart failure and death in PH across various subgroups (45–47). Additionally, a reduction in RV free wall strain has also been shown to predict worse outcomes in PH (48). Reduced strain is one of the earliest signs of RV dysfunction as patients with less longitudinal deformation had worse outcomes than matched controls with equivalent right heart dimensions and TAPSE (49, 50).

For a strain analysis to be done, 2D echo image quality must also be adequate at a frame rate of at least 70–90 frames per second. Strain imaging requires post processing using dedicated software and can be performed utilizing CMR-based techniques as well. Echo-derived strain requires specialized software and ultrasound machines, which may result in increased cost, however can typically be performed during real-time image acquisition with minimal increase in patient exam time or retrospectively on previously acquired images. There is also a significant learning curve in strain analysis as automated endocardial border definition must be verified manually by experienced operators (51). Additionally, there is well-described vendor-specific variability in strain measures (52) and the cutoff values for normal and abnormal strain also depend on the analytic software and modality, i.e., CMR vs. echo-derived strain, being used. Longitudinal strain monitoring must therefore ensure that patients' images are analyzed using the same software across time and should be performed by experienced operators.

Three-Dimensional Echocardiography

3D echocardiography is a state-of-the-art imaging strategy increasingly being used in clinical practice (53). Estimations of the RVEF have been found to be more closely correlated to those measured by CMR (54–57). However, 3D echo tends to underestimate the true RVEF (58). Despite this, the accessibility of 3D echo is greater than CMR which makes this an attractive alternative. In addition, strain imaging has been combined with 3D echo to accurately predict RVEF (59). 3D imaging can be performed during both 2D and transesophageal echocardiography and is recommended in the assessment of severe TR (60) for grading and determining suitability for intervention.

Chest Computed Tomography Imaging

Acquiring a non-contrast chest CT scan is part of the standard workup for the diagnosis of PH (10). The presence of lung disease on a chest CT along with abnormalities on pulmonary function tests can indicate PH secondary to lung disease (Group 3 PH). Along with its evaluation of the pulmonary parenchyma, there are several findings that can screen for PH on CT. These include the absolute size of the main pulmonary artery and its relative size compared to the aorta. Chest CT with contrast is also essential if acute pulmonary embolism is suspected as an etiology of PH. New CT techniques such as dual energy CT are also being investigated to measure lung perfusion qualitatively and quantitatively. A representative image from a patient with connective tissue disease- associated interstitial lung disease and mixed PH is shown in **Figure 2**.

Pulmonary Artery Size

The diameter of the main pulmonary artery (mPA) and its size in comparison to the ascending aorta correlate to mPAP on RHC. In the Framingham Heart Study, the 90th percentile for mPA diameter measured by CT was >29 mm in men and >27 mm in women (61). Subsequent work has shown that a mPA > 29 mm is correlated with elevated mPAP with a sensitivity and a specificity of ∼80% and an r of 0.6 (62–66). A ratio of the

mPA/ascending aorta >1 also correlated with elevated mPAP with ∼70% specificity and sensitivity. The mPA size can be enlarged in fibrotic lung disease which can confound its use as a screen for PH in patients with these disorders. CT has not been shown to predict PH as accurately as echo or CMR (67, 68) but its sensitivity and specificity increase when it is combined with these modalities for screening (69).

Dual Energy CT

Dual energy CT (DECT) is a technique that acquires CT angiographic (CTA) images of the pulmonary vasculature at two different energy levels after the administration of intravenous iodine-based contrast. Due to the different attenuation properties of iodine contrast at these two different energy levels, the quantity of iodine inside the pulmonary vasculature, which can serve as a surrogate for pulmonary perfusion, can be isolated and measured. As CT scans are commonly used in the work up of PH, DECT has the capability to be built into the screening chest CT without extra radiation (70). DECT is primarily used as a replacement for the V/Q scan in diagnosis of CTEPH, but has also been investigated as a screening tool for PH and a tool to assess the degree of PH. DECT has been shown to have an 80% sensitivity in the diagnosis of CTEPH compared to VQ scintigraphy (71–74) which is much improved compared to standard CTAs (75). While this is the most useful and well-understood utility of DECT, additional assessment of pulmonary perfused blood volumes (PBV), representing the total amount of iodine inside the pulmonary vasculature at a certain timepoint, can be qualitatively and quantitatively used to screen for PH. Patients with PH have a mosaic attenuation pattern on DECT given the dysregulation of the pulmonary vasculature inherent to the disease (76). Additionally, the total degree of PBV has been shown to correlate with mPAP (77) along with the ratio of PBV to the attenuation of the pulmonary artery (78, 79). However, many of these findings are non-specific.

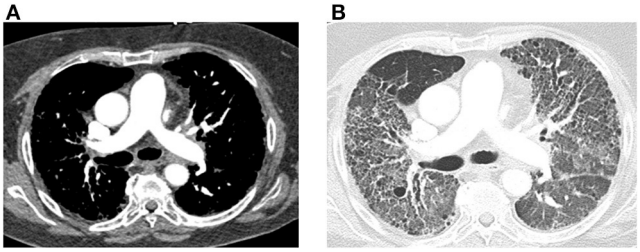

FIGURE 2 | Computed tomography (CT) images of the chest with and without contrast are shown from a 64-year-old female with connective tissue disease, severe interstitial lung disease, and mixed severe pulmonary hypertension are shown. **(A)** Transaxial images are shown demonstrating an enlarged main pulmonary arterial size at 3.2 cm when compared to ascending aorta size of 2.9 cm at the same level suggestive of pulmonary hypertension. There is no evidence of pulmonary embolism with optimal contrast opacification. **(B)** Transaxial images in the lung window demonstrate extensive bilateral diffuse groundglass opacities and honeycombing. There is associated intralobular and interstitial thickening and bronchiectasis consistent with patient's known history of connective tissue disease associated non-specific interstitial pneumonitis.

Scintigraphy and Nuclear Imaging

Ventilation-Perfusion (V/Q) Scans

V/Q Scintigraphy is part of the standardized diagnostic workup of PH, specifically for diagnosis of WHO Group 4 chronic thromboembolic pulmonary hypertension (CTEPH) (10). CTEPH is defined as PH in the presence of mismatched perfusion defects by V/Q scan as well as signs of thromboembolism on CT and/or pulmonary angiography following 3 months of therapeutic anticoagulation (10). This modality is considered to be the standard of care in the initial evaluation for PH etiologies due to high sensitivity and specificity in the diagnosis of CTEPH, outperforming CTA alone (80–82).

Nuclear Medicine Techniques

Increased stress on the right heart in PH results in an increase in myocyte glycolysis and can be measured with a radioactively tagged glucose analog and measured by PET. Increased 2-deoxy-2-[18F]fluoro-D-glucose (FDG) uptake in the RV is observed in patients with PH and correlated with mPAP (83–85). Increased FDG uptake has been found to be associated with clinical worsening and death, and patients who respond to therapy show decreased FDG uptake over time (86, 87). In addition, alternatives to FDG, such as a radiotracer targeting mannose receptors on macrophages, have been similarly observed to detect PAH and respond to pulmonary vasodilator therapy (88). Further, hybrid PET/MRI imaging has demonstrated that a combination of RV ejection fraction and tracer uptake was associated with clinical deterioration or death in PAH patients

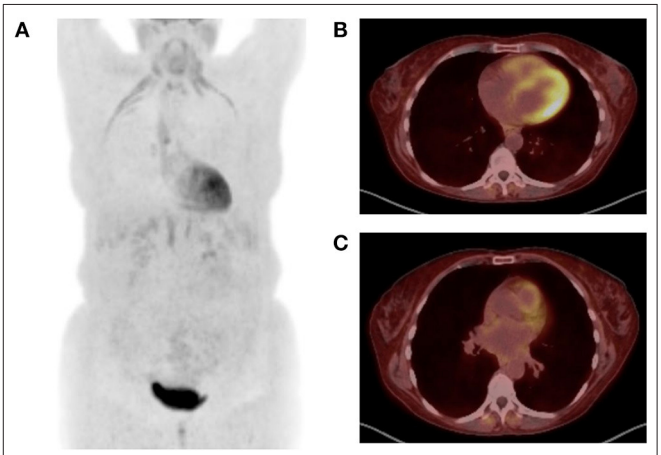

FIGURE 3 | Positron emission tomography (PET) images are shown from a 52-year-old woman with emphysema and associated Group 3 pulmonary hypertension presenting with acute exacerbation. 9.78 mCi ^{18}F-FDG injected at 119 mg/dl blood glucose level. Image acquisition 57 mins post injection. **(A)** Maximum intensity projection image demonstrates FDG uptake in the diaphragm, infrahyoid muscles, and intercostal muscles consistent with increased work of breathing noted during examination. There is also diffuse subcutaneous uptake, reflecting treatment with corticosteroids during the exacerbation. **(B)** Transaxial images at the midventricular level demonstrate abnormal uptake in the right ventricle. **(C)** Transaxial images at the level of the main pulmonary artery (mPA) demonstrate enlarged mPA and abnormal FDG uptake in the right ventricular outflow track.

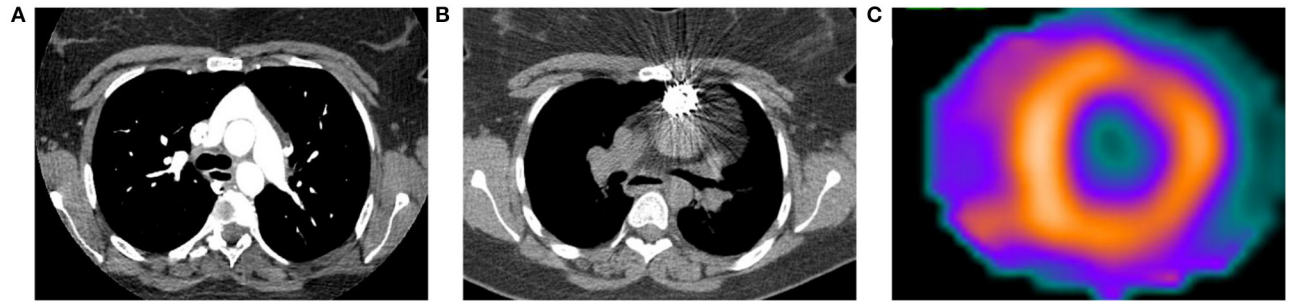

FIGURE 4 | Computed tomography (CT) and ^{99m}Tc-sestamibi single-photon emission computed tomography (SPECT) images from a 23-year-old woman with history of D-transposition of the great arteries (D-TGA) status-post repair. **(A)** Transaxial CT angiogram image demonstrating the characteristic appearance of the pulmonary artery and aorta after repair of D-TGA. **(B)** Non-contrast CT acquired at time of SPECT shows a stent in the pulmonary artery that was placed after the patient developed severe pulmonary artery stenosis. **(C)** Short axis SPECT image shows normal radiotracer distribution in the left ventricle with extension of uptake into the visualized portion of the right ventricle, consistent with pulmonary hypertension.

(89). **Figure 3** demonstrates representative FDG-PET imaging from a PH patient with emphysema.

Single-photon emission computed tomography (SPECT) utilizes multiple different radiotracers to evaluate cardiac perfusion and function. Analogous to PET, patients with PH will have evidence of thickening, enlargement, and metabolic derangement in the RV. The most commonly used radiotracers in modern cardiac SPECT are mitochondrial imaging agents (e.g., ^{99m}Tc-sestamibi), and their increased uptake in the RV is reflective of both increased RV mass and increased energy production and use (90). **Figure 4** is from a patient with a pulmonary artery stenosis and increased ^{99m}Tc-sestamibi uptake in the RV.

Cardiac Magnetic Resonance Imaging

CMR Quantitative Assessment of Structure and Function

CMR is a non-invasive, non-radiating imaging technique that allows for highly reproducible tissue characterization (90), permits assessment of radial and circumferential RV strain, and can distinguish ischemic-perfusion vs. fibrotic processes. CMR provides the best three-dimensional characterization of the RV and its dynamic relationship with the LV with high interstudy reproducibility (91). CMR also generates accurate 3D measurements of the RV throughout the cardiac cycle (92). Right ventricular mass, volume, and function can be accurately assessed and quantified on CMR. Additionally, evaluation of infiltrative disease processes relevant to development of cardiomyopathy is possible. Reduced RV ejection fraction, and RV end-systolic volume have been shown to be independent predictors of mortality (93–95). Reduced stroke volume has also been correlated with mortality (96), and improvements in stroke volume are seen in response to therapy (97, 98). Representative CMR images are demonstrated in **Figure 5**.

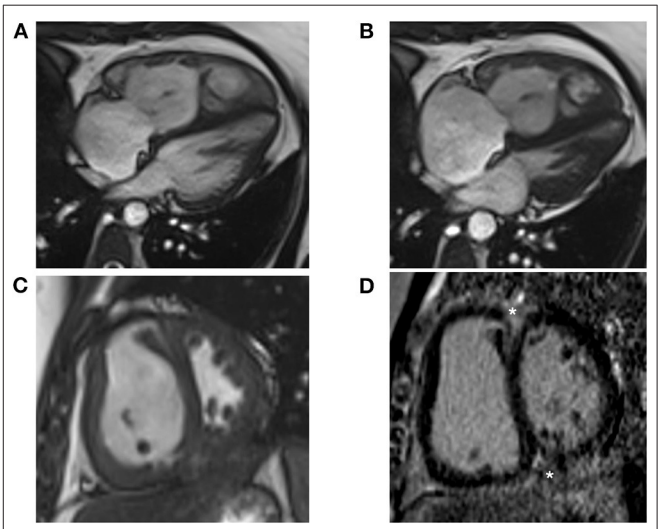

FIGURE 5 | Cardiac Magnetic Resonance (CMR) images are shown from a 38-year-old female with idiopathic pulmonary arterial hypertension. **(A)** Four-chamber bright blood CMR image from end diastole shows a dilated and hypertrophied right ventricle at a mean pulmonary pressure of 47 mmHg. End systolic images show leftward bowing of the interventricular septum from elevated right ventricular pressure. **(B)** Late systolic images show leftward bowing of the interventricular septum from elevated RV pressure. **(C)** Short axis CMR image shows marked hypertrophy of the right ventricular free wall and septal bowing. **(D)** Short axis LGE image shows prominent enhancement at the anterior and inferior RV insertion points (asterisks).

CMR Tissue Characterization and Perfusion Imaging

In the assessment of PH, CMR can be of particular value in patients with rheumatologic etiologies allowing for identification of occult lesions such as myocarditis, interstitial edema, myocardial infarction, and diffuse endocardial fibrosis (99). Assessment of native T1 and post-contrast T1 mapping allows for the accurate differentiation between the acute and chronic phases in many rheumatologic disorders. Understanding to what extent either ischemic injury or inflammation contributes to myocardial damage and fibrosis is also important in therapeutic interventions (100).

Late gadolinium enhancement (LGE) is a well validated approach for the evaluation of focal myocardial scarring and is the gold standard for *in vivo* assessment of replacement

macroscopic fibrosis (99). CMR techniques can detect fibrosis in as little as 1 cm^3 of tissue with excellent agreement with histologic studies (99, 101). Native T1 mapping and extracellular volume (ECV) quantification may be more sensitive than LGE techniques at detecting low-grade inflammation and diffuse myocardial fibrosis (102). In fact, in a recent study, rheumatologic patients were found to have higher T1 and T2 values, as well as expanded ECV compared with control subjects, with the most significant differences between native T1 and T2, independent of the presence of LGE (103). The extent and location of LGE in the RV can also indicate presence of RV stress. Delayed enhancement from gadolinium (10–20 mins after injection) is associated with cardiac fibrosis (104). Delayed enhancement mass at the insertion points of the RV is a sensitive and specific marker for PH (105–108). The extent of delayed enhancement mass into the interventricular septum is associated with worse RV function and clinical outcomes (109–111).

Quantification of myocardial perfusion utilizing CMR is observer-independent and highly reproducible (112). CMR perfusion imaging may allow for the investigation of characteristic disease-specific findings beyond the hemodynamic derangements in loading conditions in PH. In a study of CMR perfusion imaging in PAH patients associated with the autoimmune disorder systemic sclerosis (SSc-PAH) vs. those with idiopathic PAH (IPAH), RV and LV perfusion was significantly reduced and inversely correlated with RV workload and ejection fraction (113). Reduction in RV myocardial perfusion reserve was significantly correlated with worse hemodynamic profile and decreased RV function suggesting that reduced myocardial perfusion reserve may contribute to RV dysfunction in patients with PAH (113). CMR markers of RV remodeling and fibrosis, including RV and LV ventricular mass index, LGE and RV myocardial perfusion index, were also predictive of survival and improved with PAH-specific therapies.

CMR Strain Imaging

With high spatial and temporal resolution, CMR allows for quantification of global RV function across three coordinate directions (circumferential, radial, and longitudinal), as well as precise analysis of RV regional myocardial function. A variety of approaches to strain imaging with CMR are clinically available, including use of line tags and spatial modulation of magnetization (SPAMM), use of radiofrequency pulses to conduct displacement encoding with stimulated echoes (DENSE), and use of through-plane tags by strain-encoding (SENC), to name a few (114–116), although only a subset have been reliably applied to a PH population. SENC is technique with low intra- and inter-observer variabilities (117), and is based on the acquisition of two images with different frequency modulation, or low-tuning (LT) and high-tuning (HT) images in the slice-selection direction representing static and contracting tissues, respectively. Fast-SENC RV longitudinal and circumferential strain has been utilized in PH patients allowing for characterization of RV regional function with a unique pattern of reduction in RV circumferential shortening (118). Reductions in longitudinal strain correlate with RVEF and NT-proBNP in PH (119) and have a higher sensitivity and specificity to detect low RVEF when compared to circumferential strain.

Similar to STE-derived strain, CMR strain can be measured using dedicated sequences such as SENC or post-processing of cine images using feature-tracking. While CMR-derived myocardial tissue tagging and SENC have quantitative value, these modalities have not gained widespread clinical use due to expertise needed in specific sequences, additional scanning time, and the required time and cost for complex post-processing analysis (120). Ohyama et al. recently employed an alternative method of CMR strain known as multimodality tissue tracking (MTT), which similar to STE, utilizes tissue patterns obtained from cine CMR images and automatically tracks them frame to frame using an automated matching software algorithm. Findings from 30 PH patients demonstrated close correlation between MTT and SENC with high reproducibility suggesting that quantification of regional cardiac deformation using CMR cine images is feasible without the additional limitations of other CMR strain techniques. CMR and STE-basesd longitudinal strain have good inter-modality agreement while both SENC- and FT-derived circumferential strain, especially in the presence of LGE, is better detected using CMR techniques (121).

CMR Flow and PA Vasoreactivity

2D and 4D flow characterization through the RV is a novel technique to investigate the hemodynamics of the RV and pulmonary artery. CINE phase-contrast MRI can be used to quantify blood's velocity. When velocity in one direction is measured through a 2D plane it is called 2D flow MRI. However, it can underestimate the peak velocity if it is not orthogonal to the flow of interest and it cannot measure complex flow patterns with direction change. 4D flow MRI (3D CINE phase-contrast MRI) can analyze this through *post-hoc* 3D flow analysis (122). Flow through the pulmonary artery has been found to be qualitatively and quantitatively different in PH. Patients with PH have been found to have a reduced velocity of blood flow through the pulmonary artery correlating with higher pulmonary vascular resistance (123–126). The pulmonary artery is also noted to be less distensible in patients with PH, which may predict mortality (127–129). There is a greater retrograde blood flow through the PA in patients with PH (130) thought to be secondary to a turbulent vortex. The length of time of which the vortex is present during the cardiac cycle correlates with mPAP (131–133).

Endothelial dysfunction of the pulmonary vasculature is thought to be the central underlying pathophysiologic mechanism of PH and results in decreased relaxation of the PA (134). PA endothelial function is typically measured by invasive assessment of changes in PA in cross-sectional area and flow in response to an endothelial-dependent stress (135, 136). Previous work from our group utilizing the novel combination of 3T MRI methods with isometric handgrip exercise (IHE), a well-established endothelial-dependent stressor, demonstrated a non-invasive method of measuring coronary endothelial dysfunction with high reproducibility (137, 138). In recent work from our group, we demonstrated the feasibility of the

TABLE 1 | Characteristic imaging findings are summarized across imaging modalities.

Imaging modality	Characteristic findings in pulmonary hypertension
Echocardiography	**Abnormal hemodynamics**
	Right ventricular systolic pressure > 40 mmHg and/or mean pulmonary arterial pressure > 20 mmHg
	Abnormal pulmonary vascular resistance > 2 Wood Units
	Dilated inferior vena cava with or without respirophasic variation: IVC diameter ≤ 2.1 cm that collapses >50% suggests normal RAP of 3 mmHg; IVC diameter >2.1 cm that collapses <50% equivalent to RAP of 15 mmHg. In indeterminant cases, an intermediate value of 8 mmHg may be used
	Systolic flow reversal in hepatic veins suggestive of elevated right ventricular end-diastolic pressure
	Abnormal right heart chamber size and function
	Distortion of interventricular septal morphology suggestive of pressure volume overload
	Enlargement of the right atrium in chronically elevated right ventricular filling pressures
	Abnormal TAPSE ≤ 1.7 cm, tissue Doppler S' < 9.5 cm/s, fractional area change <35%
	Presence of right ventricular hypertrophy
	Globally reduced right ventricular longitudinal strain with or without regional abnormalities
	Abnormal regurgitant lesions
	Presence of pulmonary and/or tricuspid regurgitation
Chest Computed Tomography Imaging	Enlargement of main pulmonary artery in comparison to ascending aorta at same level > 1
	Evaluation of lung parenchyma which may be abnormal in Group 3 pulmonary hypertension
	Assessment for acute pulmonary embolism using contrast imaging
	Assessment of chronic thromboembolic pulmonary hypertension in Group 4 disease
Scintigraphy and Nuclear Imaging	**Abnormal Ventilation-Perfusion (VQ) Scan**
	Presence of mismatched perfusion defects by VQ scan as well as signs of thromboembolism on CT and/or pulmonary angiography following three months of therapeutic anticoagulation
	Abnormal FDG-18 uptake
	Increased FDG-18 uptake in the right ventricle and pulmonary artery
Cardiac Magnetic Resonance Imaging	**Abnormal right heart chamber size and function**
	Increased right atrial and ventricular volumes
	Abnormal interventricular septal morphology suggestive of pressure/volume overload
	Presence of right ventricular hypertrophy
	Reflux of contrast into the hepatic veins
	Decreased right ventricular function
	Abnormal CMR-derived strain along both longitudinal and circumferential axis
	Abnormal tissue characterization
	Abnormal native T1 mapping and expanded extracellular volume suggestive of tissue inflammation seen in acute phase
	Presence of late Gadolinium enhancement which can be seen at insertion points of the right ventricle and within the right and left ventricles
	Suggestive of fibrosis and tissue remodeling
	Abnormal perfusion
	Reduced right and left ventricular perfusion is inversely correlated with pulmonary pressures, and right ventricular workload and ejection fraction
	Abnormal flow and pulmonary arterial vasoreactivity
	Reduced pulmonary arterial blood flow velocity correlates with increased pulmonary vascular resistance
	Decreased pulmonary arterial distensibility
	Abnormal pulmonary artery vasoreactivity suggestive of endothelial dysfunction

non-invasive measurement of PA vasoreactivity in HIV patients with pulmonary vascular disease (139, 140).

CONCLUSION

Echocardiography, CT, nuclear imaging, and CMR are useful for non-invasively screening, classifying, prognosticating, and monitoring effectiveness of therapy in PH. Characteristic findings for each modality are further summarized in **Table 1**. The standardized algorithm using echocardiogram, CT scan, and VQ scan in the initial diagnosis and classification in PH can also be supplemented by CMR methods. While multiple modalities exist and can complement each other in the investigation of PH, a well-designed clinical approach should

account for expertise and availability of necessary imaging equipment and analytic software in a value-based framework focused on patient-specific clinical needs and prioritizing the minimization of imaging redundancy. Novel imaging techniques such as strain imaging, 3D echo, DECT, FDG-PET, and 4D flow MRI can evaluate for the severity of PH and can be used in conjunction with standard imaging modalities to monitor for disease progression and response to therapy. While RHC is the gold standard in the diagnosis and monitoring of PH, it can be supplemented by these non-invasive imaging modalities to ensure that it is selectively and appropriately used. Earlier detection of PA and RV dysfunction using these common imaging modalities can lead to earlier diagnosis and treatment of PH which has been shown to improve clinical outcomes.

AUTHOR CONTRIBUTIONS

MM was the principal investigator, had access to all the data in the study, and takes full responsibility for the integrity and accuracy of the manuscript. All authors contributed equally to the design, drafting, and final approval of this manuscript.

FUNDING

Funding for this work was supported by the American Lung Association (AB), NIH/NHLBI R01HL147660-03 (AH), NIH/NHLBI R01-HL114910 (PH), NIH/NHLBI K23-HL146889 (SH), Jerome Green Foundation (SH), Scleroderma Foundation (MM and SM), Department of Defense W81XWH2010768 (SM), and Johns Hopkins Clinician Scientist Award (MM).

REFERENCES

1. Hoeper MM, Humbert M, Souza R, Idrees M, Kawut SM, Sliwa-Hahnle K, et al. A global view of pulmonary hypertension. *Lancet Respir Med.* (2016) 4:306–22. doi: 10.1016/S2213-2600(15)00543-3
2. Wijeratne DT, Lajkosz K, Brogly SB, Lougheed MD, Jiang L, Housin A, et al. Increasing incidence and prevalence of World Health Organization Groups 1 to 4 pulmonary hypertension: a population-based cohort study in Ontario, Canada. *Circ Cardiovasc Qual Outcomes.* (2018) 11:e003973. doi: 10.1161/CIRCOUTCOMES.117.003973
3. Gall H, Felix JF, Schneck FK, Milger K, Sommer N, Voswinckel R, et al. The Giessen Pulmonary Hypertension Registry: survival in pulmonary hypertension subgroups. *J Heart Lung Transplant.* (2017) 36:957–67. doi: 10.1016/j.healun.2017.02.016
4. Humbert M, Yaici A, de Groote P, Montani D, Sitbon O, Launay D, et al. Screening for pulmonary arterial hypertension in patients with systemic sclerosis: clinical characteristics at diagnosis and long-term survival. *Arthritis Rheum.* (2011) 63:3522–30. doi: 10.1002/art.30541
5. Deaño RC, Glassner-Kolmin C, Rubenfire M, Frost A, Visovatti S, McLaughlin VV, et al. Referral of patients with pulmonary hypertension diagnoses to tertiary pulmonary hypertension centers: the multicenter RePHerral study. *JAMA Intern Med.* (2013) 173:887–93. doi: 10.1001/jamainternmed.2013.319
6. Brown LM, Chen H, Halpern S, Taichman D, McGoon MD, Farber HW, et al. Delay in recognition of pulmonary arterial hypertension: factors identified from the REVEAL Registry. *Chest.* (2011) 140:19–26. doi: 10.1378/chest.10-1166
7. Simonneau G, Montani D, Celermajer DS, Denton CP, Gatzoulis MA, Krowka M, et al. Haemodynamic definitions and updated clinical classification of pulmonary hypertension. *Eur Respir J.* (2019) 53:1801913. doi: 10.1183/13993003.01913-2018
8. Simonneau G, Hoeper MM. The revised definition of pulmonary hypertension: exploring the impact on patient management. *Eur Heart J Suppl.* (2019) 21(Suppl K):K4–8. doi: 10.1093/eurheartj/suz211
9. Hoeper MM, Lee SH, Voswinckel R, Palazzini M, Jais X, Marinelli A, et al. Complications of right heart catheterization procedures in patients with pulmonary hypertension in experienced centers. *J Am Coll Cardiol.* (2006) 48:2546–52. doi: 10.1016/j.jacc.2006.07.061
10. Galiè N, Humbert M, Vachiery J-L, Gibbs S, Lang I, Torbicki A, et al. 2015 ESC/ERS Guidelines for the diagnosis and treatment of pulmonary hypertension: The Joint Task Force for the Diagnosis and Treatment of Pulmonary Hypertension of the European Society of Cardiology (ESC) and the European Respiratory Society (ERS): Endorsed by: Association for European Paediatric and Congenital Cardiology (AEPC), International Society for Heart and Lung Transplantation (ISHLT). *Eur Respir J.* (2015) 46:903–75. doi: 10.1183/13993003.01032-2015
11. Pearlman AS, Ryan T, Picard MH, Douglas PS. Evolving trends in the use of echocardiography: a study of Medicare beneficiaries. *J Am Coll Cardiol.* (2007) 49:2283–91. doi: 10.1016/j.jacc.2007.02.048
12. Berger M, Haimowitz A, Van Tosh A, Berdoff RL, Goldberg E. Quantitative assessment of pulmonary hypertension in patients with tricuspid regurgitation using continuous wave Doppler ultrasound. *J Am Coll Cardiol.* (1985) 6:359–65. doi: 10.1016/S0735-1097(85)80172-8
13. Rudski LG, Lai WW, Afilalo J, Hua L, Handschumacher MD, Chandrasekaran K, et al. Guidelines for the echocardiographic assessment of the right heart in adults: a report from the American Society of Echocardiography. *Journal of the American Society of Echocardiography.* (2010) 23:685–713. doi: 10.1016/j.echo.2010.05.010
14. Strange G, Playford D, Stewart S, Deague JA, Nelson H, Kent A, et al. Pulmonary hypertension: prevalence and mortality in the Armadale echocardiography cohort. *Heart.* (2012) 98:1805–11. doi: 10.1136/heartjnl-2012-301992
15. Fisher MR, Forfia PR, Chamera E, Housten-Harris T, Champion HC, Girgis RE, et al. Accuracy of Doppler echocardiography in the hemodynamic assessment of pulmonary hypertension. *Am J Respir Crit Care Med.* (2009) 179:615–21. doi: 10.1164/rccm.200811-1691OC
16. Yin D, Wang Y, Zheng M, Wei H, Li M, Lv T, et al. Comparison of pulmonary artery pressure measurement with Doppler echocardiography or with right heart catheterization in patients with congenital heart disease. *Front Pediatr.* (2019) 7:421. doi: 10.3389/fped.2019.00421
17. Nathan SD, Shlobin OA, Barnett SD, Saggar R, Belperio JA, Ross DJ, et al. Right ventricular systolic pressure by echocardiography as a predictor of pulmonary hypertension in idiopathic pulmonary fibrosis. *Respir Med.* (2008) 102:1305–10. doi: 10.1016/j.rmed.2008.03.022
18. Fisher MR, Criner GJ, Fishman AP, Hassoun PM, Minai OA, Scharf SM, et al. Estimating pulmonary artery pressures by echocardiography in patients with emphysema. *Eur Respir J.* (2007) 30:914–21. doi: 10.1183/09031936.00033007
19. Borgeson DD, Seward JB, Miller FA, Oh JK, Tajik AJ. Frequency of Doppler measurable pulmonary artery pressures. *J Am Soc Echocardiogr.* (1996) 9:832–7. doi: 10.1016/S0894-7317(96)90475-7
20. Coghlan JG, Denton CP, Grünig E, Bonderman D, Distler O, Khanna D, et al. Evidence-based detection of pulmonary arterial hypertension in systemic sclerosis: the DETECT study. *Ann Rheum Dis.* (2014) 73:1340–9. doi: 10.1136/annrheumdis-2013-203301
21. Takahama H, McCully RB, Frantz RP, Kane GC. Unraveling the RV ejection doppler envelope: insight into pulmonary artery hemodynamics and disease severity. *JACC Cardiovasc Imaging.* (2017) 10(10 Pt B):1268–77. doi: 10.1016/j.jcmg.2016.12.021
22. Do DH, Therrien J, Marelli A, Martucci G, Afilalo J, Sebag IA. Right atrial size relates to right ventricular end-diastolic pressure in an adult population with congenital heart disease. *Echocardiography.* (2011) 28:109–16. doi: 10.1111/j.1540-8175.2010.01277.x

23. Lai WW, Gauvreau K, Rivera ES, Saleeb S, Powell AJ, Geva T. Accuracy of guideline recommendations for two-dimensional quantification of the right ventricle by echocardiography. *Int J Cardiovasc Imaging.* (2008) 24:691–8. doi: 10.1007/s10554-008-9314-4
24. Lang RM, Badano LP, Mor-Avi V, Afilalo J, Armstrong A, Ernande L, et al. Recommendations for cardiac chamber quantification by echocardiography in adults: an update from the American Society of Echocardiography and the European Association of Cardiovascular Imaging. *J Am Soc Echocardiogr.* (2015) 28:1–39.e14. doi: 10.1016/j.echo.2014.10.003
25. Kossaify A. Echocardiographic assessment of the right ventricle, from the conventional approach to speckle tracking and three-dimensional imaging, and insights into the "right way" to explore the forgotten chamber. *Clin Med Insights Cardiol.* (2015) 9:65–75. doi: 10.4137/CMC.S27462
26. Li Y, Wang Y, Zhai Z, Guo X, Yang Y, Lu X. Real-time three-dimensional echocardiography to assess right ventricle function in patients with pulmonary hypertension. *PLoS ONE.* (2015) 10:e0129557. doi: 10.1371/journal.pone.0129557
27. Gripari P, Muratori M, Fusini L, Tamborini G, Ali SG, Brusoni D, et al. Right ventricular dimensions and function: why do we need a more accurate and quantitative imaging? *J Cardiovasc Echogr.* (2015) 25:19–25. doi: 10.4103/2211-4122.158420
28. Modin D, Møgelvang R, Andersen DM, Biering-Sørensen T. Right ventricular function evaluated by tricuspid annular plane systolic excursion predicts cardiovascular death in the general population. *J Am Heart Assoc.* (2019) 8:e012197. doi: 10.1161/JAHA.119.012197
29. Sato T, Tsujino I, Ohira H, Oyama-Manabe N, Yamada A, Ito YM, et al. Validation study on the accuracy of echocardiographic measurements of right ventricular systolic function in pulmonary hypertension. *J Am Soc Echocardiogr.* (2012) 25:280–6. doi: 10.1016/j.echo.2011.12.012
30. Hsiao S-H, Lin S-K, Wang W-C, Yang S-H, Gin P-L, Liu C-P. Severe tricuspid regurgitation shows significant impact in the relationship among peak systolic tricuspid annular velocity, tricuspid annular plane systolic excursion, and right ventricular ejection fraction. *J Am Soc Echocardiogr.* (2006) 19:902–10. doi: 10.1016/j.echo.2006.01.014
31. Tei C, Dujardin KS, Hodge DO, Bailey KR, McGoon MD, Tajik AJ, et al. Doppler echocardiographic index for assessment of global right ventricular function. *J Am Soc Echocardiogr.* (1996) 9:838–47. doi: 10.1016/S0894-7317(96)90476-9
32. Tei C, Nishimura RA, Seward JB, Tajik AJ. Noninvasive Doppler-derived myocardial performance index: Correlation with simultaneous measurements of cardiac catheterization measurements. *J Am Soc Echocardiogr.* (1997) 10:169–78. doi: 10.1016/S0894-7317(97)70090-7
33. Lindqvist P, Waldenström A, Henein M, Mörner S, Kazzam E. Regional and global right ventricular function in healthy individuals aged 20-90 years: a pulsed Doppler tissue imaging study: Umeå General Population Heart Study. *Echocardiography.* (2005) 22:305–14. doi: 10.1111/j.1540-8175.2005.04023.x
34. Kylhammar D, Kjellström B, Hjalmarsson C, Jansson K, Nisell M, Söderberg S, et al. A comprehensive risk stratification at early follow-up determines prognosis in pulmonary arterial hypertension. *Eur Heart J.* (2018) 39:4175–81. doi: 10.1093/eurheartj/ehx257
35. Grünig E, Tiede H, Enyimayew EO, Ehlken N, Seyfarth H-J, Bossone E, et al. Assessment and prognostic relevance of right ventricular contractile reserve in patients with severe pulmonary hypertension. *Circulation.* (2013) 128:2005–15. doi: 10.1161/CIRCULATIONAHA.113.001573
36. Kane GC, Maradit-Kremers H, Slusser JP, Scott CG, Frantz RP, McGoon MD. Integration of clinical and hemodynamic parameters in the prediction of long-term survival in patients with pulmonary arterial hypertension. *Chest.* (2011) 139:1285–93. doi: 10.1378/chest.10-1293
37. Benza RL, Gomberg-Maitland M, Elliott CG, Farber HW, Foreman AJ, Frost AE, et al. Predicting survival in patients with pulmonary arterial hypertension: the REVEAL Risk Score Calculator 2.0 and comparison with ESC/ERS-based risk assessment strategies. *Chest.* (2019) 156:323–37. doi: 10.1016/j.chest.2019.02.004
38. Batal O, Dardari Z, Costabile C, Gorcsan J, Arena VC, Mathier MA. Prognostic value of pericardial effusion on serial echocardiograms in pulmonary arterial hypertension. *Echocardiography.* (2015) 32:1471–6. doi: 10.1111/echo.12909
39. Mathai SC, Suber T, Khair RM, Kolb TM, Damico RL, Hassoun PM. Health-related quality of life and survival in pulmonary arterial hypertension. *Ann Am Thorac Soc.* (2016) 13:31–9. doi: 10.1513/AnnalsATS.201412-572OC
40. Forfia PR, Fisher MR, Mathai SC, Housten-Harris T, Hemnes AR, Borlaug BA, et al. Tricuspid annular displacement predicts survival in pulmonary hypertension. *Am J Respir Crit Care Med.* (2006) 174:1034–41. doi: 10.1164/rccm.200604-547OC
41. Sebbag I, Rudski LG, Therrien J, Hirsch A, Langleben D. Effect of chronic infusion of epoprostenol on echocardiographic right ventricular myocardial performance index and its relation to clinical outcome in patients with primary pulmonary hypertension. *Am J Cardiol.* (2001) 88:1060–3. doi: 10.1016/S0002-9149(01)01995-6
42. Lee J-H, Park J-H. Strain analysis of the right ventricle using two-dimensional echocardiography. *J Cardiovasc Imaging.* (2018) 26:111–24. doi: 10.4250/jcvi.2018.26.e11
43. Simon MA, Rajagopalan N, Mathier MA, Shroff SG, Pinsky MR, López-Candales A. Tissue Doppler imaging of right ventricular decompensation in pulmonary hypertension. *Congest Heart Fail.* (2009) 15:271–6. doi: 10.1111/j.1751-7133.2009.00113.x
44. Meris A, Faletra F, Conca C, Klersy C, Regoli F, Klimusina J, et al. Timing and magnitude of regional right ventricular function: a speckle tracking-derived strain study of normal subjects and patients with right ventricular dysfunction. *J Am Soc Echocardiogr.* (2010) 23:823–31. doi: 10.1016/j.echo.2010.05.009
45. Shukla M, Park J-H, Thomas JD, Delgado V, Bax JJ, Kane GC, et al. Prognostic value of right ventricular strain using speckle-tracking echocardiography in pulmonary hypertension: a systematic review and meta-analysis. *Can J Cardiol.* (2018) 34:1069–78. doi: 10.1016/j.cjca.2018.04.016
46. Haeck MLA, Scherptong RWC, Marsan NA, Holman ER, Schalij MJ, Bax JJ, et al. Prognostic value of right ventricular longitudinal peak systolic strain in patients with pulmonary hypertension. *Circ Cardiovasc Imaging.* (2012) 5:628–36. doi: 10.1161/CIRCIMAGING.111.971465
47. Fine NM, Chen L, Bastiansen PM, Frantz RP, Pellikka PA, Oh JK, et al. Outcome prediction by quantitative right ventricular function assessment in 575 subjects evaluated for pulmonary hypertension. *Circ Cardiovasc Imaging.* (2013) 6:711–21. doi: 10.1161/CIRCIMAGING.113.000640
48. Sachdev A, Villarraga HR, Frantz RP, McGoon MD, Hsiao J-F, Maalouf JF, et al. Right ventricular strain for prediction of survival in patients with pulmonary arterial hypertension. *Chest.* (2011) 139:1299–309. doi: 10.1378/chest.10-2015
49. Mukherjee M, Mercurio V, Tedford RJ, Shah AA, Hsu S, Mullin CJ, et al. Right ventricular longitudinal strain is diminished in systemic sclerosis compared with idiopathic pulmonary arterial hypertension. *Eur Resp J.* (2017) 50:1701436. doi: 10.1183/13993003.01436-2017
50. Mukherjee M, Chung S-E, Ton Von K, Tedford RJ, Hummers LK, Wigley FM, et al. Unique abnormalities in right ventricular longitudinal strain in systemic sclerosis patients. *Circul Cardiovasc Imaging.* (2016) 9:e003792. doi: 10.1161/CIRCIMAGING.115.003792
51. Chan J, Shiino K, Obonyo NG, Hanna J, Chamberlain R, Small A, et al. Left ventricular global strain analysis by two-dimensional speckle-tracking echocardiography: the learning curve. *J Am Soc Echocardiogr.* (2017) 30:1081–90. doi: 10.1016/j.echo.2017.06.010
52. Farsalinos KE, Daraban AM, Ünlü S, Thomas JD, Badano LP, Voigt J-U. Head-to-head comparison of global longitudinal strain measurements among nine different vendors: the EACVI/ASE inter-vendor comparison study. *J Am Soc Echocardiogr.* (2015) 28:1171–81.e2. doi: 10.1016/j.echo.2015.06.011
53. Tamborini G, Brusoni D, Torres Molina JE, Galli CA, Maltagliati A, Muratori M, et al. Feasibility of a new generation three-dimensional echocardiography for right ventricular volumetric and functional measurements. *Am J Cardiol.* (2008) 102:499–505. doi: 10.1016/j.amjcard.2008.03.084
54. Jenkins C, Chan J, Bricknell K, Strudwick M, Marwick TH. Reproducibility of right ventricular volumes and ejection fraction using real-time three-dimensional echocardiography: comparison with cardiac MRI. *Chest.* (2007) 131:1844–51. doi: 10.1378/chest.06-2143
55. Leibundgut G, Rohner A, Grize L, Bernheim A, Kessel-Schaefer A, Bremerich J, et al. Dynamic assessment of right ventricular volumes and function by real-time three-dimensional echocardiography: a comparison study with

magnetic resonance imaging in 100 adult patients. *J Am Soc Echocardiogr.* (2010) 23:116–26. doi: 10.1016/j.echo.2009.11.016
56. Shimada YJ, Shiota M, Siegel RJ, Shiota T. Accuracy of right ventricular volumes and function determined by three-dimensional echocardiography in comparison with magnetic resonance imaging: a meta-analysis study. *J Am Soc Echocardiogr.* (2010) 23:943–53. doi: 10.1016/j.echo.2010.06.029
57. Morikawa T, Murata M, Okuda S, Tsuruta H, Iwanaga S, Murata M, et al. Quantitative analysis of right ventricular function in patients with pulmonary hypertension using three-dimensional echocardiography and a two-dimensional summation method compared to magnetic resonance imaging. *Am J Cardiol.* (2011) 107:484–9. doi: 10.1016/j.amjcard.2010.09.047
58. Khoo NS, Young A, Occleshaw C, Cowan B, Zeng ISL, Gentles TL. Assessments of right ventricular volume and function using three-dimensional echocardiography in older children and adults with congenital heart disease: comparison with cardiac magnetic resonance imaging. *J Am Soc Echocardiogr.* (2009) 22:1279–88. doi: 10.1016/j.echo.2009.08.011
59. Smith BCF, Dobson G, Dawson D, Charalampopoulos A, Grapsa J, Nihoyannopoulos P. Three-dimensional speckle tracking of the right ventricle: toward optimal quantification of right ventricular dysfunction in pulmonary hypertension. *J Am Coll Cardiol.* (2014) 64:41–51. doi: 10.1016/j.jacc.2014.01.084
60. Otto CM, Nishimura RA, Bonow RO, Carabello BA, Erwin JP, Gentile F, et al. 2020 ACC/AHA guideline for the management of patients with valvular heart disease: executive summary: a report of the American College of Cardiology/American Heart Association Joint Committee on Clinical Practice Guidelines. *Circulation.* (2021) 143:e35–71. doi: 10.1161/CIR.0000000000000932
61. Truong QA, Massaro JM, Rogers IS, Mahabadi AA, Kriegel MF, Fox CS, et al. Reference values for normal pulmonary artery dimensions by noncontrast cardiac computed tomography: the Framingham Heart Study. *Circ Cardiovasc Imaging.* (2012) 5:147–54. doi: 10.1161/CIRCIMAGING.111.968610
62. Mahammedi A, Oshmyansky A, Hassoun PM, Thiemann DR, Siegelman SS. Pulmonary artery measurements in pulmonary hypertension: the role of computed tomography. *J Thorac Imaging.* (2013) 28:96–103. doi: 10.1097/RTI.0b013e318271c2eb
63. Kam JC, Pi J, Doraiswamy V, Elnahar Y, Abdul-Jawad S, DeBari VA, et al. CT scanning in the evaluation of pulmonary hypertension. *Lung.* (2013) 191:321–6. doi: 10.1007/s00408-013-9464-6
64. Chan AL, Juarez MM, Shelton DK, MacDonald T, Li C-S, Lin T-C, et al. Novel computed tomographic chest metrics to detect pulmonary hypertension. *BMC Med Imaging.* (2011) 11:7. doi: 10.1186/1471-2342-11-7
65. Shen Y, Wan C, Tian P, Wu Y, Li X, Yang T, et al. CT-base pulmonary artery measurement in the detection of pulmonary hypertension: a meta-analysis and systematic review. *Medicine.* (2014) 93:e256. doi: 10.1097/MD.0000000000000256
66. Tan RT, Kuzo R, Goodman LR, Siegel R, Haasler GB, Presberg KW. Utility of CT scan evaluation for predicting pulmonary hypertension in patients with parenchymal lung disease. Medical College of Wisconsin Lung Transplant Group. *Chest.* (1998) 113:1250–6. doi: 10.1378/chest.113.5.1250
67. Devaraj A, Wells AU, Meister MG, Corte TJ, Hansell DM. The effect of diffuse pulmonary fibrosis on the reliability of CT signs of pulmonary hypertension. *Radiology.* (2008) 249:1042–9. doi: 10.1148/radiol.2492080269
68. Rajaram S, Swift AJ, Capener D, Elliot CA, Condliffe R, Davies C, et al. Comparison of the diagnostic utility of cardiac magnetic resonance imaging, computed tomography, and echocardiography in assessment of suspected pulmonary arterial hypertension in patients with connective tissue disease. *J Rheumatol.* (2012) 39:1265–74. doi: 10.3899/jrheum.110987
69. Devaraj A, Wells AU, Meister MG, Corte TJ, Wort SJ, Hansell DM. Detection of pulmonary hypertension with multidetector CT and echocardiography alone and in combination. *Radiology.* (2010) 254:609–16. doi: 10.1148/radiol.09090548
70. Thieme SF, Johnson TRC, Reiser MF, Nikolaou K. Dual-energy lung perfusion computed tomography: a novel pulmonary functional imaging method. *Semin Ultrasound CT MR.* (2010) 31:301–8. doi: 10.1053/j.sult.2010.05.001
71. Dournes G, Verdier D, Montaudon M, Bullier E, Rivière A, Dromer C, et al. Dual-energy CT perfusion and angiography in chronic thromboembolic pulmonary hypertension: diagnostic accuracy and concordance with radionuclide scintigraphy. *Eur Radiol.* (2014) 24:42–51. doi: 10.1007/s00330-013-2975-y
72. Nakazawa T, Watanabe Y, Hori Y, Kiso K, Higashi M, Itoh T, et al. Lung perfused blood volume images with dual-energy computed tomography for chronic thromboembolic pulmonary hypertension: correlation to scintigraphy with single-photon emission computed tomography. *J Comput Assist Tomogr.* (2011) 35:590–5. doi: 10.1097/RCT.0b013e318224e227
73. Thieme SF, Becker CR, Hacker M, Nikolaou K, Reiser MF, Johnson TRC. Dual energy CT for the assessment of lung perfusion–correlation to scintigraphy. *Eur J Radiol.* (2008) 68:369–74. doi: 10.1016/j.ejrad.2008.07.031
74. Koike H, Sueyoshi E, Sakamoto I, Uetani M, Nakata T, Maemura K. Comparative clinical and predictive value of lung perfusion blood volume CT, lung perfusion SPECT and catheter pulmonary angiography images in patients with chronic thromboembolic pulmonary hypertension before and after balloon pulmonary angioplasty. *Eur Radiol.* (2018) 28:5091–9. doi: 10.1007/s00330-018-5501-4
75. Pitton MB, Kemmerich G, Herber S, Schweden F, Mayer E, Thelen M. Chronic thromboembolic pulmonary hypertension: diagnostic impact of Multislice-CT and selective Pulmonary-DSA. *Rofo.* (2002) 174:474–9. doi: 10.1055/s-2002-25117
76. Hoey ETD, Mirsadraee S, Pepke-Zaba J, Jenkins DP, Gopalan D, Screaton NJ. Dual-energy CT angiography for assessment of regional pulmonary perfusion in patients with chronic thromboembolic pulmonary hypertension: initial experience. *AJR Am J Roentgenol.* (2011) 196:524–32. doi: 10.2214/AJR.10.4842
77. Meinel FG, Graef A, Thierfelder KM, Armbruster M, Schild C, Neurohr C, et al. Automated quantification of pulmonary perfused blood volume by dual-energy CTPA in chronic thromboembolic pulmonary hypertension. *Rofo.* (2014) 186:151–6. doi: 10.1055/s-0033-1350412
78. Ameli-Renani S, Ramsay L, Bacon JL, Rahman F, Nair A, Smith V, et al. Dual-energy computed tomography in the assessment of vascular and parenchymal enhancement in suspected pulmonary hypertension. *J Thorac Imaging.* (2014) 29:98–106. doi: 10.1097/RTI.0000000000000061
79. Koike H, Sueyoshi E, Sakamoto I, Uetani M, Nakata T, Maemura K. Quantification of lung perfusion blood volume (lung PBV) by dual-energy CT in patients with chronic thromboembolic pulmonary hypertension (CTEPH) before and after balloon pulmonary angioplasty (BPA): Preliminary results. *Eur J Radiol.* (2016) 85:1607–12. doi: 10.1016/j.ejrad.2016.06.016
80. Tunariu N, Gibbs SJR, Win Z, Gin-Sing W, Graham A, Gishen P, et al. Ventilation-perfusion scintigraphy is more sensitive than multidetector CTPA in detecting chronic thromboembolic pulmonary disease as a treatable cause of pulmonary hypertension. *J Nucl Med.* (2007) 48:680–4. doi: 10.2967/jnumed.106.039438
81. He J, Fang W, Lv B, He J-G, Xiong C-M, Liu Z-H, et al. Diagnosis of chronic thromboembolic pulmonary hypertension: comparison of ventilation/perfusion scanning and multidetector computed tomography pulmonary angiography with pulmonary angiography. *Nucl Med Commun.* (2012) 33:459–63. doi: 10.1097/MNM.0b013e32835085d9
82. Furfaro D, Azadi J, Housten T, Kolb TM, Damico RL, Hassoun PM, et al. Discordance between imaging modalities in the evaluation of chronic thromboembolic pulmonary hypertension: a combined experience from two academic medical centers. *Ann ATS.* (2019) 16:277–80. doi: 10.1513/AnnalsATS.201809-588RL
83. Wang L, Li W, Yang Y, Wu W, Cai Q, Ma X, et al. Quantitative assessment of right ventricular glucose metabolism in idiopathic pulmonary arterial hypertension patients: a longitudinal study. *Eur Heart J Cardiovasc Imaging.* (2016) 17:1161–8. doi: 10.1093/ehjci/jev297
84. Oikawa M, Kagaya Y, Otani H, Sakuma M, Demachi J, Suzuki J, et al. Increased [18F]fluorodeoxyglucose accumulation in right ventricular free wall in patients with pulmonary hypertension and the effect of epoprostenol. *J Am Coll Cardiol.* (2005) 45:1849–55. doi: 10.1016/j.jacc.2005.02.065
85. Saygin D, Highland KB, Farha S, Park M, Sharp J, Roach EC, et al. Metabolic and functional evaluation of the heart and lungs in pulmonary hypertension by gated 2-[18F]-Fluoro-2-deoxy-D-glucose positron emission tomography. *Pulm Circ.* (2017) 7:428–38. doi: 10.1177/2045893217701917

86. Tatebe S, Fukumoto Y, Oikawa-Wakayama M, Sugimura K, Satoh K, Miura Y, et al. Enhanced [18F]fluorodeoxyglucose accumulation in the right ventricular free wall predicts long-term prognosis of patients with pulmonary hypertension: a preliminary observational study. *Eur Heart J Cardiovasc Imaging.* (2014) 15:666–72. doi: 10.1093/ehjci/jet276
87. Fang W, Zhao L, Xiong C-M, Ni X-H, He Z-X, He J-G, et al. Comparison of 18F-FDG uptake by right ventricular myocardium in idiopathic pulmonary arterial hypertension and pulmonary arterial hypertension associated with congenital heart disease. *Pulm Circ.* (2012) 2:365–72. doi: 10.4103/2045-8932.101651
88. Park J-B, Suh M, Park JY, Park JK, Kim Y, Kim H, et al. Assessment of inflammation in pulmonary artery hypertension by ^{68} Ga-Mannosylated human serum albumin. *Am J Respir Crit Care Med.* (2020) 201:95–106. doi: 10.1164/rccm.201903-0639OC
89. Kazimierczyk R, Szumowski P, Nekolla SG, Blaszczak P, Malek LA, Milosz-Wieczorek B, et al. Prognostic role of PET/MRI hybrid imaging in patients with pulmonary arterial hypertension. *Heart.* (2021) 107:54–60. doi: 10.1136/heartjnl-2020-316741
90. Mannting F, Zabrodina YV, Dass C. Significance of increased right ventricular uptake on 99mTc-Sestamibi SPECT in patients with coronary artery disease. *J Nuclear Med.* (1999) 40:889–94.
91. Mavrogeni S, Sfikakis PP, Gialafos E, Bratis K, Karabela G, Stavropoulos E, et al. Cardiac tissue characterization and the diagnostic value of cardiovascular magnetic resonance in systemic connective tissue diseases. *Arthritis Care Res.* (2014) 66:104–12. doi: 10.1002/acr.22181
92. Grothues F, Moon JC, Bellenger NG, Smith GS, Klein HU, Pennell DJ. Interstudy reproducibility of right ventricular volumes, function, and mass with cardiovascular magnetic resonance. *Am Heart J.* (2004) 147:218–23. doi: 10.1016/j.ahj.2003.10.005
93. Kawel-Boehm N, Maceira A, Valsangiacomo-Buechel ER, Vogel-Claussen J, Turkbey EB, Williams R, et al. Normal values for cardiovascular magnetic resonance in adults and children. *J Cardiovasc Magn Reson.* (2015) 17:29. doi: 10.1186/s12968-015-0111-7
94. Swift AJ, Rajaram S, Campbell MJ, Hurdman J, Thomas S, Capener D, et al. Prognostic value of cardiovascular magnetic resonance imaging measurements corrected for age and sex in idiopathic pulmonary arterial hypertension. *Circ Cardiovasc Imaging.* (2014) 7:100–6. doi: 10.1161/CIRCIMAGING.113.000338
95. Swift AJ, Capener D, Johns C, Hamilton N, Rothman A, Elliot C, et al. Magnetic resonance imaging in the prognostic evaluation of patients with pulmonary arterial hypertension. *Am J Respir Crit Care Med.* (2017) 196:228–39. doi: 10.1164/rccm.201611-2365OC
96. Baggen VJM, Leiner T, Post MC, van Dijk AP, Roos-Hesselink JW, Boersma E, et al. Cardiac magnetic resonance findings predicting mortality in patients with pulmonary arterial hypertension: a systematic review and meta-analysis. *Eur Radiol.* (2016) 26:3771–80. doi: 10.1007/s00330-016-4217-6
97. van Wolferen SA, Marcus JT, Boonstra A, Marques KMJ, Bronzwaer JGF, Spreeuwenberg MD, et al. Prognostic value of right ventricular mass, volume, and function in idiopathic pulmonary arterial hypertension. *Eur Heart J.* (2007) 28:1250–7. doi: 10.1093/eurheartj/ehl477
98. Peacock AJ, Crawley S, McLure L, Blyth KG, Vizza CD, Poscia R, et al. Changes in right ventricular function measured by cardiac magnetic resonance imaging in patients receiving pulmonary arterial hypertension-targeted therapy: the EURO-MR study. *Circ Cardiovasc Imaging.* (2014) 7:107–14. doi: 10.1161/CIRCIMAGING.113.000629
99. van Wolferen SA, van de Veerdonk MC, Mauritz G-J, Jacobs W, Marcus JT, Marques KMJ, et al. Clinically significant change in stroke volume in pulmonary hypertension. *Chest.* (2011) 139:1003–9. doi: 10.1378/chest.10-1066
100. Mavrogeni SI, Schwitter J, Gargani L, Pepe A, Monti L, Allanore Y, et al. Cardiovascular magnetic resonance in systemic sclerosis: "Pearls and pitfalls." Semin Arthritis Rheum (2017) 47(1):79–85. doi: 10.1016/j.semarthrit.2017.03.020
101. Mavrogeni S, Markousis-Mavrogenis G, Koutsogeorgopoulou L, Dimitroulas T, Bratis K, Kitas GD, et al. Cardiovascular magnetic resonance imaging pattern at the time of diagnosis of treatment naïve patients with connective tissue diseases. *Int J Cardiol.* (2017) 236:151–6. doi: 10.1016/j.ijcard.2017.01.104
102. Barison A, Gargani L, De Marchi D, Aquaro GD, Guiducci S, Picano E, et al. Early myocardial and skeletal muscle interstitial remodelling in systemic sclerosis: insights from extracellular volume quantification using cardiovascular magnetic resonance. *Eur Heart J Cardiovasc Imaging.* (2015) 16:74–80. doi: 10.1093/ehjci/jeu167
103. Ntusi NAB, Piechnik SK, Francis JM, Ferreira VM, Rai ABS, Matthews PM, et al. Subclinical myocardial inflammation and diffuse fibrosis are common in systemic sclerosis–a clinical study using myocardial T1-mapping and extracellular volume quantification. *J Cardiovasc Magn Reson.* (2014) 16:21. doi: 10.1186/1532-429X-16-21
104. Mayr A, Kitterer D, Latus J, Steubing H, Henes J, Vecchio F, et al. Evaluation of myocardial involvement in patients with connective tissue disorders: a multi-parametric cardiovascular magnetic resonance study. *J Cardiovasc Magn Reson.* (2016) 18:67. doi: 10.1186/s12968-016-0288-4
105. Bessa LGP, Junqueira FP, Bandeira ML da S, Garcia MI, Xavier SS, Lavall G, et al. Pulmonary arterial hypertension: use of delayed contrast-enhanced cardiovascular magnetic resonance in risk assessment. *Arq Bras Cardiol.* (2013) 101:336–43. doi: 10.5935/abc.20130168
106. Shehata ML, Lossnitzer D, Skrok J, Boyce D, Lechtzin N, Mathai SC, et al. Myocardial delayed enhancement in pulmonary hypertension: pulmonary hemodynamics, right ventricular function, and remodeling. *AJR Am J Roentgenol.* (2011) 196:87–94. doi: 10.2214/AJR.09.4114
107. Sanz J, Dellegrottaglie S, Kariisa M, Sulica R, Poon M, O'Donnell TP, et al. Prevalence and correlates of septal delayed contrast enhancement in patients with pulmonary hypertension. *Am J Cardiol.* (2007) 100:731–5. doi: 10.1016/j.amjcard.2007.03.094
108. Junqueira FP, Macedo R, Coutinho AC, Loureiro R, De Pontes PV, Domingues RC, et al. Myocardial delayed enhancement in patients with pulmonary hypertension and right ventricular failure: evaluation by cardiac MRI. *Br J Radiol.* (2009) 82:821–6. doi: 10.1259/bjr/28241773
109. Freed BH, Gomberg-Maitland M, Chandra S, Mor-Avi V, Rich S, Archer SL, et al. Late gadolinium enhancement cardiovascular magnetic resonance predicts clinical worsening in patients with pulmonary hypertension. *J Cardiovasc Magn Reson.* (2012) 14:11. doi: 10.1186/1532-429X-14-11
110. Swift AJ, Rajaram S, Capener D, Elliot C, Condliffe R, Wild JM, et al. LGE patterns in pulmonary hypertension do not impact overall mortality. *JACC Cardiovasc Imaging.* (2014) 7:1209–17. doi: 10.1016/j.jcmg.2014.08.014
111. Blyth KG, Groenning BA, Martin TN, Foster JE, Mark PB, Dargie HJ, et al. Contrast enhanced-cardiovascular magnetic resonance imaging in patients with pulmonary hypertension. *Eur Heart J.* (2005) 26:1993–9. doi: 10.1093/eurheartj/ehi328
112. McCann GP, Gan CT, Beek AM, Niessen HWM, Vonk Noordegraaf A, van Rossum AC. Extent of MRI delayed enhancement of myocardial mass is related to right ventricular dysfunction in pulmonary artery hypertension. *AJR Am J Roentgenol.* (2007) 188:349–55. doi: 10.2214/AJR.05.1259
113. Rodríguez-Reyna TS, Morelos-Guzman M, Hernández-Reyes P, Montero-Duarte K, Martínez-Reyes C, Reyes-Utrera C, et al. Assessment of myocardial fibrosis and microvascular damage in systemic sclerosis by magnetic resonance imaging and coronary angiotomography. *Rheumatology (Oxford).* (2015) 54:647–54. doi: 10.1093/rheumatology/keu350
114. Vogel-Claussen J, Skrok J, Shehata ML, Singh S, Sibley CT, Boyce DM, et al. Right and left ventricular myocardial perfusion reserves correlate with right ventricular function and pulmonary hemodynamics in patients with pulmonary arterial hypertension. *Radiology.* (2011) 258:119–27. doi: 10.1148/radiol.10100725
115. Scatteia A, Baritussio A, Bucciarelli-Ducci C. Strain imaging using cardiac magnetic resonance. *Heart Fail Rev.* (2017) 22:465–76. doi: 10.1007/s10741-017-9621-8
116. Ibrahim E-SH. Myocardial tagging by Cardiovascular Magnetic Resonance: evolution of techniques–pulse sequences, analysis algorithms, and applications. *J Cardiovasc Magn Reson.* (2011) 13:36. doi: 10.1186/1532-429X-13-36
117. Auger DA, Zhong X, Epstein FH, Spottiswoode BS. Mapping right ventricular myocardial mechanics using 3D cine DENSE cardiovascular magnetic resonance. *J Cardiovasc Magn Reson.* (2012) 14:4. doi: 10.1186/1532-429X-14-4
118. Youssef A, Ibrahim E-SH, Korosoglou G, Abraham MR, Weiss RG, Osman NF. Strain-encoding cardiovascular magnetic resonance for assessment

of right-ventricular regional function. *J Cardiovasc Magn Reson.* (2008) 10:33. doi: 10.1186/1532-429X-10-33
119. Shehata ML, Basha TA, Tantawy WH, Lima JA, Vogel-Claussen J, Bluemke DA, et al. Real-time single-heartbeat fast strain-encoded imaging of right ventricular regional function: normal versus chronic pulmonary hypertension. *Magn Reson Med.* (2010) 64:98–106. doi: 10.1002/mrm.22408
120. Oyama-Manabe N, Sato T, Tsujino I, Kudo K, Manabe O, Kato F, et al. The strain-encoded (SENC) MR imaging for detection of global right ventricular dysfunction in pulmonary hypertension. *Int J Cardiovasc Imaging.* (2013) 29:371–8. doi: 10.1007/s10554-012-0105-6
121. Ohyama Y, Ambale-Venkatesh B, Chamera E, Shehata ML, Corona-Villalobos CP, Zimmerman SL, et al. Comparison of strain measurement from multimodality tissue tracking with strain-encoding MRI and harmonic phase MRI in pulmonary hypertension. *Int J Cardiol.* (2015) 182:342–8. doi: 10.1016/j.ijcard.2015.01.016
122. Erley J, Genovese D, Tapaskar N, Alvi N, Rashedi N, Besser SA, et al. Echocardiography and cardiovascular magnetic resonance based evaluation of myocardial strain and relationship with late gadolinium enhancement. *J Cardiovasc Magn Reson.* (2019) 21:46. doi: 10.1186/s12968-019-0559-y
123. Bollache E, van Ooij P, Powell A, Carr J, Markl M, Barker AJ. Comparison of 4D flow and 2D velocity-encoded phase contrast MRI sequences for the evaluation of aortic hemodynamics. *Int J Cardiovasc Imaging.* (2016) 32:1529–41. doi: 10.1007/s10554-016-0938-5
124. Ley S, Mereles D, Puderbach M, Gruenig E, Schöck H, Eichinger M, et al. Value of MR phase-contrast flow measurements for functional assessment of pulmonary arterial hypertension. *Eur Radiol.* (2007) 17:1892–7. doi: 10.1007/s00330-006-0559-9
125. Mousseaux E, Tasu JP, Jolivet O, Simonneau G, Bittoun J, Gaux JC. Pulmonary arterial resistance: noninvasive measurement with indexes of pulmonary flow estimated at velocity-encoded MR imaging–preliminary experience. *Radiology.* (1999) 212:896–902. doi: 10.1148/radiology.212.3.r99au21896
126. Barker AJ, Roldán-Alzate A, Entezari P, Shah SJ, Chesler NC, Wieben O, et al. Four-dimensional flow assessment of pulmonary artery flow and wall shear stress in adult pulmonary arterial hypertension: results from two institutions. *Magn Reson Med.* (2015) 73:1904–13. doi: 10.1002/mrm.25326
127. Ohno Y, Hatabu H, Murase K, Higashino T, Nogami M, Yoshikawa T, et al. Primary pulmonary hypertension: 3D dynamic perfusion MRI for quantitative analysis of regional pulmonary perfusion. *AJR Am J Roentgenol.* (2007) 188:48–56. doi: 10.2214/AJR.05.0135
128. Sanz J, Kariisa M, Dellegrottaglie S, Prat-González S, Garcia MJ, Fuster V, et al. Evaluation of pulmonary artery stiffness in pulmonary hypertension with cardiac magnetic resonance. *JACC Cardiovasc Imaging.* (2009) 2:286–95. doi: 10.1016/j.jcmg.2008.08.007
129. Bogren HG, Klipstein RH, Mohiaddin RH, Firmin DN, Underwood SR, Rees RS, et al. Pulmonary artery distensibility and blood flow patterns: a magnetic resonance study of normal subjects and of patients with pulmonary arterial hypertension. *Am Heart J.* (1989) 118(5 Pt 1):990–9. doi: 10.1016/0002-8703(89)90235-4
130. Gan CT-J, Lankhaar J-W, Westerhof N, Marcus JT, Becker A, Twisk JWR, et al. Noninvasively assessed pulmonary artery stiffness predicts mortality in pulmonary arterial hypertension. *Chest.* (2007) 132:1906–12. doi: 10.1378/chest.07-1246
131. Kondo C, Caputo GR, Masui T, Foster E, O'Sullivan M, Stulbarg MS, et al. Pulmonary hypertension: pulmonary flow quantification and flow profile analysis with velocity-encoded cine MR imaging. *Radiology.* (1992) 183:751–8. doi: 10.1148/radiology.183.3.1584932
132. Reiter G, Reiter U, Kovacs G, Kainz B, Schmidt K, Maier R, et al. Magnetic resonance-derived 3-dimensional blood flow patterns in the main pulmonary artery as a marker of pulmonary hypertension and a measure of elevated mean pulmonary arterial pressure. *Circ Cardiovasc Imaging.* (2008) 1:23–30. doi: 10.1161/CIRCIMAGING.108.780247
133. Reiter U, Reiter G, Kovacs G, Stalder AF, Gulsun MA, Greiser A, et al. Evaluation of elevated mean pulmonary arterial pressure based on magnetic resonance 4D velocity mapping: comparison of visualization techniques. *PLoS ONE.* (2013) 8:e82212. doi: 10.1371/journal.pone.0082212
134. Reiter G, Reiter U, Kovacs G, Olschewski H, Fuchsjäger M. Blood flow vortices along the main pulmonary artery measured with MR imaging for diagnosis of pulmonary hypertension. *Radiology.* (2015) 275:71–9. doi: 10.1148/radiol.14140849
135. Budhiraja R, Tuder RM, Hassoun PM. Endothelial dysfunction in pulmonary hypertension. *Circulation.* (2004) 109:159–65. doi: 10.1161/01.CIR.0000102381.57477.50
136. Apitz C, Zimmermann R, Kreuder J, Jux C, Latus H, Pons-Kühnemann J, et al. Assessment of pulmonary endothelial function during invasive testing in children and adolescents with idiopathic pulmonary arterial hypertension. *J Am Coll Cardiol.* (2012) 60:157–64. doi: 10.1016/j.jacc.2012.04.010
137. Flammer AJ, Anderson T, Celermajer DS, Creager MA, Deanfield J, Ganz P, et al. The assessment of endothelial function: from research into clinical practice. *Circulation.* (2012) 126:753–67. doi: 10.1161/CIRCULATIONAHA.112.093245
138. Hays AG, Iantorno M, Soleimanifard S, Steinberg A, Schär M, Gerstenblith G, et al. Coronary vasomotor responses to isometric handgrip exercise are primarily mediated by nitric oxide: a noninvasive MRI test of coronary endothelial function. *Am J Physiol Heart Circ Physiol.* (2015) 308:H1343–1350. doi: 10.1152/ajpheart.00023.2015
139. Hays AG, Hirsch GA, Kelle S, Gerstenblith G, Weiss RG, Stuber M. Noninvasive visualization of coronary artery endothelial function in healthy subjects and in patients with coronary artery disease. *J Am Coll Cardiol.* (2010) 56:1657–65. doi: 10.1016/j.jacc.2010.06.036
140. Goerlich E, Mukherjee M, Schar M, Brown TT, Bonanno G, Weiss RG, et al. Noninvasive detection of impaired pulmonary artery endothelial function in people living with HIV. *AIDS.* (2020) 34:2231–8. doi: 10.1097/QAD.0000000000002671

Conflict of Interest: The authors declare that the research was conducted in the absence of any commercial or financial relationships that could be construed as a potential conflict of interest.